LWT - Food Science and Technology 167 (2022) 113859

Contents lists available at ScienceDirect

LWT

journal homepage: www.elsevier.com/locate/lwt

Effect of particle characteristics and foaming parameters on resulting foam quality and stability

Ramona Rüegg [a,*], Tamara Schmid [a], Lukas Hollenstein [b], Nadina Müller [a]

[a] Zurich University of Applied Sciences, Institute of Food and Beverage Innovation, Einsiedlerstrasse 29, 8820, Wädenswil, Switzerland
[b] Zurich University of Applied Sciences, Institute of Computational Life Sciences, Schloss 1, 8820, Wädenswil, Switzerland

ARTICLE INFO

Keywords:
Food foams
Particle properties
Shear rate
Gas fraction
Median bubble size
Drainage

ABSTRACT

In this study, the effects of ten different food-grade particles on bubble quality and stabilization of particle-stabilized food foams in batch and continuous foaming with and without polyglycerol ester (PGE) as an emulsifier were investigated. Particle properties, such as contact angle and porosity, and varying process parameters, such as shear rate and gas fraction, were assessed with respect to their impact on bubble size $x_{50,0}$, bubble size distribution width and drainage.

The smallest bubble size $x_{50,0}$ in foams without PGE could be achieved with banana powder (88 μm), calcium carbonate (89 μm) and microcrystalline cellulose (79 μm) particles. In comparison, the smallest size in the reference without particles were 105 μm. Combining the use of particles with PGE further reduced bubble size by up to 57% and drainage by up to 100%. Increasing the shear rate from 4922 s^{-1} (35 μm) to 9844 s^{-1} (14 μm) resulted in smaller mean bubble sizes and significantly narrower bubble size distributions whereas no distinct correlation between gas fraction and resulting bubble size was found.

This study shows that using suitable particles in combination with an optimized foaming process promotes both bubble quality and the stability of foams.

1. Introduction

Particle-stabilized foams have been shown to have extraordinary stability due to a close-packed layer of particles at the gas-liquid interface (Du et al., 2003; Kostakis, Ettelaie, & Murray, 2007). Examples of foamed food products that are partially or fully stabilized by particles are foamed ice cream or foamed dairy products (E, Pei, & Schmidt, 2010). There are examples from non-food applications like dried and sintered particle based ceramic foams which prove the ability of particle-based foams to survive drying processes (Gonzenbach, Studart, Tervoort, & Gauckler, 2006). However, no applications in the field of baked products have been published in scientific literature or patents. Nevertheless, there is a clear potential for the multiplication of this approach in a variety of baked goods, from breads to pastries. Since the principles of particle-stabilized foams in food and non-food applications are comparable and some food applications already exist, a transfer of this technique to a wider range of food applications would be desirable.

Understanding the influence of food-grade particles' properties on foam stability and quality is an indispensable part of developing suitable liquid foams for foods. The choice of particles is limited compared to particles used in material science, especially in terms of raw material, adaptation of surface properties and particle size. As a metastable system, a liquid foam is subject to various ageing reactions such as liquid leakage (drainage) due to the capillary pressure gradient in the continuous phase (Hutzler, Weaire, Saugey, Cox, & Peron, 2005, October), disproportionation as a result of the Laplace pressure difference and gas diffusion velocity (Saint-Jalmes, 2006) and coalescence caused by breaks in the liquid film between the bubbles (Colin, 2012). These ageing reactions often occur simultaneously and to a certain extent influence each other (Colin, 2012; Koehler, 2012). To achieve foam stabilization using particles, the particles must have a high adsorption rate and the stabilized interfaces must have increased viscoelasticity to be able to counteract mechanical forces (Langevin, 2000). The effectiveness of these factors is determined by various particle properties such as:

(i) Optimal particle size: Small particles increase the packing density but adsorption is weaker due to the lower adsorption energy (Stocco, Rio, Binks, & Langevin, 2011). As a result, the optimum particle size is recipe dependent. Usually, ten-fold smaller mean particle sizes than the desired bubble size are preferred. (Aktas,

* Corresponding author.
E-mail address: ramona.rueegg@zhaw.ch (R. Rüegg).

https://doi.org/10.1016/j.lwt.2022.113859
Received 11 March 2022; Received in revised form 12 May 2022; Accepted 6 August 2022
Available online 10 August 2022

Cilliers, & Banford, 2008; Alargova, Panov & Velev, 2004; Binks & Horozov, 2005; Costa, Gomes, Tobolla, Menegalli & Cunha, 2018; Dickinson, 2015; Fujii, Iddon, Ryan, & Armes, 2006; Gonzenbach et al., 2006; Tang, Xiao, Tang, & Jiang, 1989). For foams, particle size is limited to sizes in the high nanometer to micrometer range. Such low values are however difficult to achieve in most materials.

(ii) Polarity and wetting angle (θP): Particles interact with bubbles according to their wetting angle (θP) at the gas-liquid interface. Since more hydrophobic particles have a destabilizing effect on foams, less hydrophobic particles with a resulting wetting angle of $\leq 90°$ are predominantly used for foam stabilization (Fameau & Salonen, 2014; Stocco et al., 2011). The wetting angle also affects the necessary adsorption energy, i.e. particles with a wetting angle of around 90° require considerably more energy to adsorb and to detach from the bubble surface than particles with smaller ($\theta P < 30°$) wetting angles (Binks, 2002).

(iii) Shape and form factors: Different particle shapes, such as spheres (Tang et al., 1989), microrods (Alargova, Warhadpande, Paunov, & Velev, 2004), cellulose fibres (Costa, Gomes, Tibolla, Menegalli, & Cunha, 2018), platelets (Guevara et al., 2012) or ellipsoids (Madivala, Vandebril, Fransaer & Vermant., 2009) can be suitable for foam stabilization. However, their shapes can influence both the packing density of the particles at the boundary layer and their interaction with each other. It is assumed that fibrous particles become entangled with each other, forming aggregates that can form a network. Such aggregates are capable of binding hydrate water, which in turn results in an increased viscosity of the continuous phase. Such network formations have been shown to be efficient in preventing coalescence of oil in water pickering emulsions (Kalashnikova, Bizot, Bertoncini, Cathala, & Capron, 2013).

A better understanding of the change in structure and stability of foams produced with different particles, different foaming devices and varying foaming parameters is expected to help promote highly stable particle-stabilized foams as additives in a wide range of food products. This is especially important in light of the fact that while particles result in particularly high foam stability (Dickinson, 2012; Stocco, Drenckhan, Rio, Langevin, & Binks, 2009), the stabilization of the air-liquid interfaces is slower than for emulsifier stabilized foams, for which a decrease in interfacial tension sometimes coupled with electrostatic repulsion results in fast stabilization (Rayner, 2015). This is an important factor in continuous foam production where interfaces need to be stabilized very quickly because bubble formation times are in the range of milliseconds and overall residence times in the foaming head are in the range of seconds. Therefore, the combination of a fast-acting emulsifier with slower-acting particles is expected to yield superior results. For this reason, the current study aimed to investigate the dependence of foam quality on a) different particle properties through the screening of various particles b) different shear forces and rates using three different foaming machines and c) varying gas fractions dispersed at different shear rates in a foaming unit. This is important in food applications where foams are subjected to physical or thermal stress in down-stream processing such as transport in pipes, kneading, drying of meringues or in foam-mat drying.

2. Material and methods

2.1. Preparation of basic suspensions with and without polyglycerol ester

For the basic suspension (continuous phase), 3% milk protein (Emmi Milchprotein 85%, Emmi AG, Lucerne, Switzerland) and 0.3% guar gum (Guar gum, Pacovis AG, Stetten, Switzerland) were dispersed in 45 °C warm tap water (96.7%) at 5500 rpm for 90 s using a rotor-stator disperser (Chemcol-Ytron, MS1 CAA-R, Ytron F. Mundwiler & Co. AG, Rüschlikon, Switzerland). For the basic suspension with the polyglycerol ester (PGE) stabilizer, 1% PGE (GRINDSTED® PGE 55 MB, Dupont Nutrition Biosciences ApS, Grindsted, Denmark) was stirred into 95 °C water (95.7%), the water was cooled to 45 °C and then 3% milk protein and 0.3% guar gum were dispersed as above. The prepared suspensions were left to rest overnight at 4 °C. After resting and just before foaming, the respective particles were dispersed to reach a concentration of 3% of the total mass for 90 s at a shear rate of 69 s^{-1} with a disperser (Chemcol-Ytron, MS1 CAA-R, Ytron F. Mundwiler & Co. AG, Rüschlikon, Switzerland).

2.2. Foaming for particle screening

For particle screening purposes, the following particles were examined in the basic suspension, both with and without PGE: silicic acid (Kieselsäure Lebensmittelqualität, Armonia GmbH, Switzerland), oil press cake from golden linseed (Bio Goldlein Presskuchen, Goldmühle GmbH, Switzerland), oil press cake from sunflower seeds (Bio Sonnenblumen Presskuchen, Goldmühle GmbH, Switzerland), soy protein isolate (Soya Protein Isolate 100% unflavoured, bulk, UK), microcrystalline cellulose (Microcrystalline Cellulose, J. Rettenmaier & Söhne, Germany), banana powder (Bananenfruchtpulver, Spiceworld GmbH, Austria), pea protein isolate (Super Pea Protein Isolate, bulk, UK), calcium carbonate (Calcipur 110 KP, Omya AG, Switzerland), soy granulate (Vantastic Foods Soja Granulat, hellovegan, Switzerland) and chicken egg white (Egg White Powder, bulk, UK).

600g of the basic suspension was whisked in a kitchen foaming machine (Hob-N50 Universal food processor, Hobart) for 4 min at the highest rotational speed (agitator = 580 rpm). The foamed basic suspensions with (Ref_PGE) and without PGE (Ref_w) were prepared and served as reference foams. All experiments were carried out in duplicate.

2.3. Foaming with different foaming machines

To observe the influence of different foaming machines on foam quality, microcrystalline cellulose particles were added to the basic suspension with PGE as described in 2.1. The mixture was then foamed using a rotor-stator foaming machine (MEGATRON® MT-FM 50 Pilot-Plant, Kinematica AG, Malters, Switzerland) or a membrane foaming machine (MEGATRON® MT-MM 1–55, Kinematica AG, Malters, Switzerland). For the foaming machine (MT-FM), the Radax double T-pin geometry 50/6 was used, for the membrane foaming machine (MT-MM) a sinter membrane with an average pore size of 2 μm and a gap width of 2 mm was used. During foaming with both the MT-FM and the MT-MM, the total flow rate (continuous phase and gas input) was kept constant at 0.4 L/min and the product outlet temperature was kept at 20–25 °C. A gas input of 0.5 theoretical gas fraction was dispersed in the foaming heads of the MT-FM and the MT-MM using shear rates of 9844 s^{-1} and 4869 s^{-1}, respectively. The foamed basic suspensions without particles (Ref_w) and without particles but with PGE (Ref_PGE) served as reference foams. All experiments were carried out in duplicate.

2.4. Foaming with different parameters

To evaluate the influence of different foaming parameters, microcrystalline cellulose particles, banana powder and oil press cake from golden linseed were added to the basic suspension with PGE as described in section 2.1. The mixtures were then foamed using a rotor-stator foaming machine MT-FM with the Radax double T-pin geometry configuration 50/6. During foaming, the total flow rate was kept constant at 0.6 L/min and the product outlet temperature was kept at 20–25 °C. Gas inputs of 0.25, 0.5 and 0.62 theoretical gas fraction were dispersed in the foaming head using rotor speeds of 4922, 7383 and 9844 s^{-1}, respectively. The foamed basic suspension without particles but with PGE (Ref_PGE) served as a reference foam. All experiments were carried out in duplicate and foams in which blowby was generated

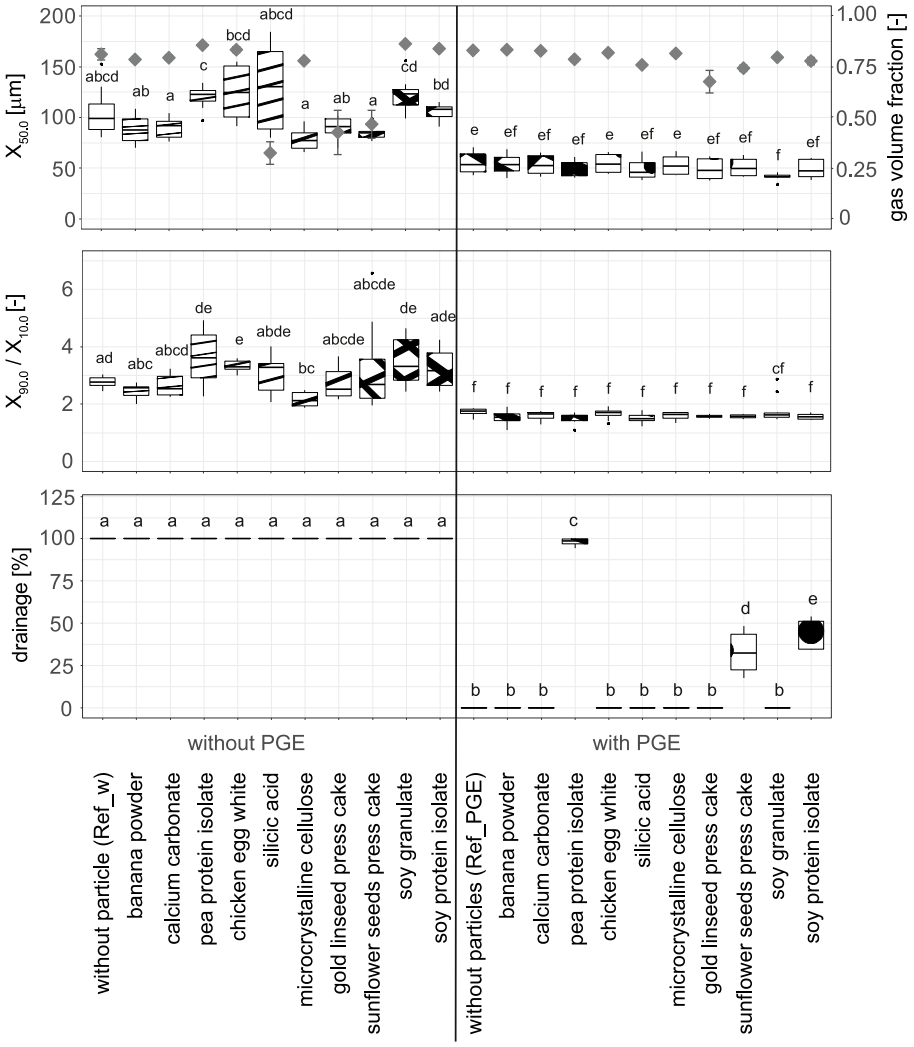

Fig. 1. Top panel: bubble size $x_{50.0}$ [µm] (boxes, left axis, n = 12) and gas fraction Θ_V [−] achieved directly after foaming (diamonds ◆, right axis, n = 6). Center panel: bubble size distribution width $x_{90.0}/x_{10.0}$ [-], n = 12. Bottom panel: drainage [%] after 24 h (100% drainage = no foam left), n = 6. Foams were made with a kitchen whipping machine (Hobart) in duplicate, with and without the PGE emulsifier and stabilized with different particles. Letters (a, b, …) indicate classes of significance based on the analysis through a Kruskal-Wallis test (α = 0.05) followed by an unpaired Wilcoxon test using statistical software (RStudio V 1.4 1717, Boston MA, US).

were discarded.

2.5. Analyses

2.5.1. Gas fraction

Effectively achieved gas fraction $Ø_V$ was calculated using the following the formula:

$$Ø_V\,[-] = \frac{\frac{OR\ [\%]}{100}}{\frac{OR\ [\%]}{100} + 1} \qquad \text{(Eq. 1)}$$

where the Overrun (OR) was determined gravimetrically by measuring the density of the product both immediately before (ρ_{liquid}) and immediately after foaming (ρ_{Foam}) using the following formula:

$$OR\ [\%] = \frac{\rho_{liquid}\left[\frac{kg}{m3}\right] - \rho_{foam}\left[\frac{kg}{m3}\right]}{\rho_{foam}\left[\frac{kg}{m3}\right]} \cdot 100\ \ \% \qquad \text{(Eq. 2)}$$

Analysis was determined in triplicate for each repetition to achieve a minimum total number of values of n = 6 per experimental setup.

2.5.2. Bubble size distribution

Micrographs of each foam were taken for all experiments using an inverted light microscope (RLV-100-G, Discover Echo Inc., San Diego, United States) directly after foaming (t0) and after 24 h (t24) to determine the influence of foaming parameters on foam stability. Images were taken at either 4x, 10x or 20x magnification to achieve a minimum of 50 bubbles and a maximum of 1000 bubbles per image. The micrographs were analyzed using the BubbleAnalyser© software (ZHAW internal application), which binarized the image using a dynamic threshold set at the 15% darkest pixels followed by an edge finding algorithm. The BubbleAnalyser© software was validated against long established analyzing software BubbleDetect© (Copyright 2003 Lab of Food Process Engineering (LMVT), ETH Zurich, Switzerland, Müller--Fischer, Bleuler, & Windhab, 2007). Cumulative number distribution functions were then derived from the resulting contour diameters and the median bubble diameter $x_{50,0}$ as well as distribution width $x_{90,0}/x_{10,0}$ was quantified. Six micrographs of each foam were taken to achieve a total number of values of n = 12.

2.5.3. Drainage

The drainage of the foams was measured in a cup with a volume scale (5 ml steps from 0 to 120 ml) after 24 h (t24) and converted into a percentage of the total weight. Analysis was performed in triplicate to achieve a total number of values of n = 6.

2.5.4. Influence of particle properties and foaming parameters on foam quality

To evaluate the influence of different particle properties and foaming parameters on the bubble size $x_{50.0}$ and the bubble distribution width $x_{90.0}/x_{10.0}$, microcrystalline cellulose particles, banana powder and oil

press cake from golden linseed were analyzed. Part of the analysis took place in external, accredited laboratories: (i) mean particle size [μm] and particle distribution width [$x_{90.0}/x_{10.0}$] by means of microscopic analysis, (ii) the Brunauer-Emmett-Teller (BET) method for measuring the surface area using helium pyknometry, (iii) circularity (roundish, flat) and surface texture (smooth, rough) using microscopy. In addition, the wetting angle [°] was analyzed by pressing particles into dense tablets (n = 6) using a tablet press (MTQX-1, GlobePharma, USA), adding a defined droplet of water to the surface and quantifying the contact angle (Contact Angle System OCA Goniometer, dataphysics, Germany).

2.5.5. Statistical evaluation

For statistical analysis, the data for bubble size distribution and drainage were subjected to a Kruskal-Wallis test (α = 0.05) followed by an unpaired Wilcoxon test using statistical software (RStudio V April 1, 1717, RStudio PBC, Boston MA, United States).

3. Results and discussion

3.1. Influence of different particles and PGE on foam quality

It was observed that the use of PGE in the base mix significantly reduced the average bubble size and its variance compared to the samples without PGE (Fig. 1). Likewise, the width of the bubble size distribution $x_{90.0}/x_{10.0}$ was reduced by 35% on average by the addition of the PGE emulsifier. For example, the reference sample without PGE (Ref_w) had a distribution width of around 2.3, while this was reduced to 1.6 (−27%) in the reference sample with PGE. However, for the samples with PGE, no significant differences between the effects of different particles on bubble size $x_{50,0}$ could be detected. The results show that the use of the fast-acting PGE emulsifier overrides any impact of different particles on bubble size $x_{50.0}$ (Hunter, Pugh, Franks, & Jameson, 2008; Kapatay & Babcsán, 2012). This is not unexpected, since the resulting bubbles size in such a low shear system is primarily dominated by the fast stabilization of the bubble interfaces.

None of the particle stabilized foams produced without PGE differed significantly from the reference without particles (Ref_w) in terms of bubble size $x_{50.0}$ (Fig. 1). However, the screening of the different particles tested with the base mix without PGE showed that both the bubble size $x_{50.0}$ and the distribution width $x_{90.0}/x_{10.0}$ can be greatly reduced, depending on the particle chosen (Fig. 1). For example, the bubble size and bubble size distribution width of the chicken egg white particle foam (125.0 μm and 43.34) were a factor of 1.6 higher and 1.5 wider than that produced with microcrystalline cellulose (78.6 μm and 2.17). The five smallest median bubble sizes $x_{50,0}$ without PGE were achieved with the banana powder, calcium carbonate, microcrystalline cellulose, oil press cake golden linseed and oil press cake sunflower seeds particles. The significant differences between individual particles might be attributed to different particle properties, such as size, shape, wetting angle, density, and chemical composition.

After 24 h, all of the foams without PGE, regardless of the particles used, were completely separated (=100% drainage) (Fig. 1). It is assumed that the interfacial adsorption of the particles was not sufficiently strong on its own. Furthermore, according to Kaptay (2003), who recommends aiming for a maximum bubble size of 3 μm, the initial gas bubbles were simply too large for long-term stabilization of the foam system. In the foams with PGE and pea protein isolate, sunflower press cake and soy protein isolate, significant drainage of 98%, 33% and 44% was observed after 24 h. All the other foams with PGE remained extremely stable and showed no drainage (=0%), even after 24 h. It is not possible to say whether the particles contributed additionally to the stability of these foams due to interactions between particles and the PGE molecules as found by other researchers (Hunter et al., 2008; Kapatay & Babcsán, 2012). Likewise, oleosins present in press cakes (Rayner, 2015) as well as fat crystals (Ho, Le, Yan, Bhandari, & Bansal, 2019), proteins and fibers present in the particles may also have triggered additional stabilization reactions and interactions (Martínez-Flores et al., 2006; Rayner, 2015). Fibrous materials in particular are known to form aggregates which are capable of binding hydrate water, resulting in an increased viscosity of the continuous phase. Such network formations have been shown to be efficient in preventing coalescence (Kalashnikova et al., 2013).

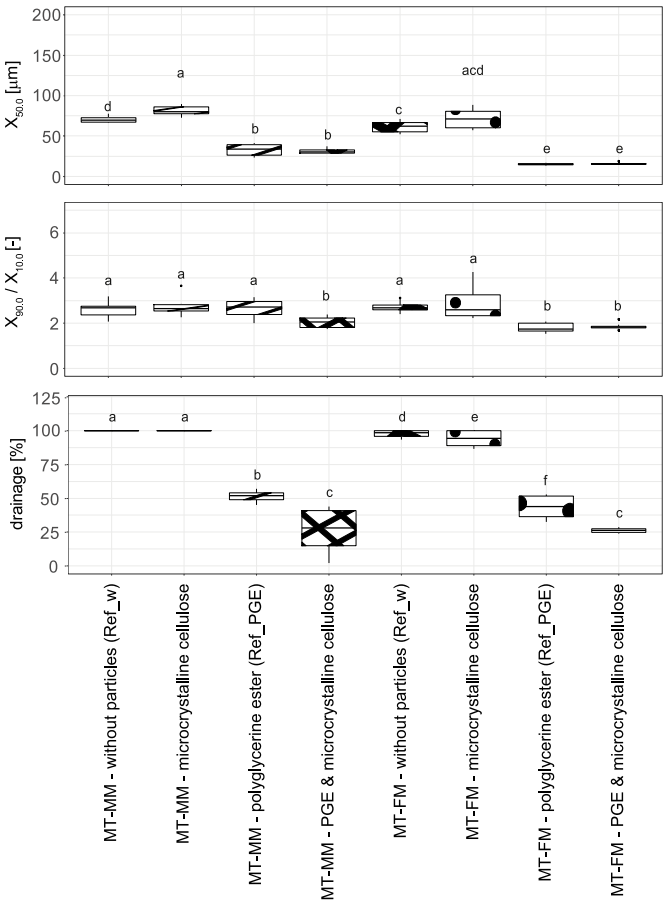

Fig. 2. Top panel: bubble size $x_{50.0}$ [μm], n = 12. Center panel: bubble size distribution width $x_{90.0}/x_{10.0}$ [-] directly after foaming, n = 12. Bottom panel: drainage [%] after 24 h (100% drainage = no foam left), n = 6. Foams were made with and without the PGE emulsifier, stabilized with microcrystalline cellulose particles, and foamed with either a rotor-membrane foaming machine (MT-MM) or a rotor-stator foaming machine (MT-FM) in duplicate. Letters (a, b, …) indicate classes of significance based on the analysis through a Kruskal-Wallis test (α = 0.05) followed by an unpaired Wilcoxon test using statistical software (RStudio V 1.4 1717, Boston MA, US).

The gas fraction obtained was high for all of the samples tested, ranging between 0.68 and 0.86. The only exceptions were the foams with the basic mix formulation without PGE, which were stabilized with silicic acid (Θ_V 0.32), golden linseed press cake (Θ_V 0.42) and sunflower seed press cake (Θ_V 0.47) particles (Fig. 1). The lower gas uptake ratios of these foams might be due to the lower foaming capacity of the proteins present and their limited ability to form stable networks. However, the gas fraction achieved had no obvious influence on bubble quality or foam stability.

Particle properties were not tested, since the decision criteria for screening were result-based, i.e. particles with minimum bubble size $x_{50,0}$, smallest size distribution and lowest drainage rate were selected for in-depth follow-up study. In addition, off-smells, such as for foams produced with silicic acid were also discarded. Based on these criteria, the microcrystalline cellulose, banana powder and gold linseed press cake particles were rated the best.

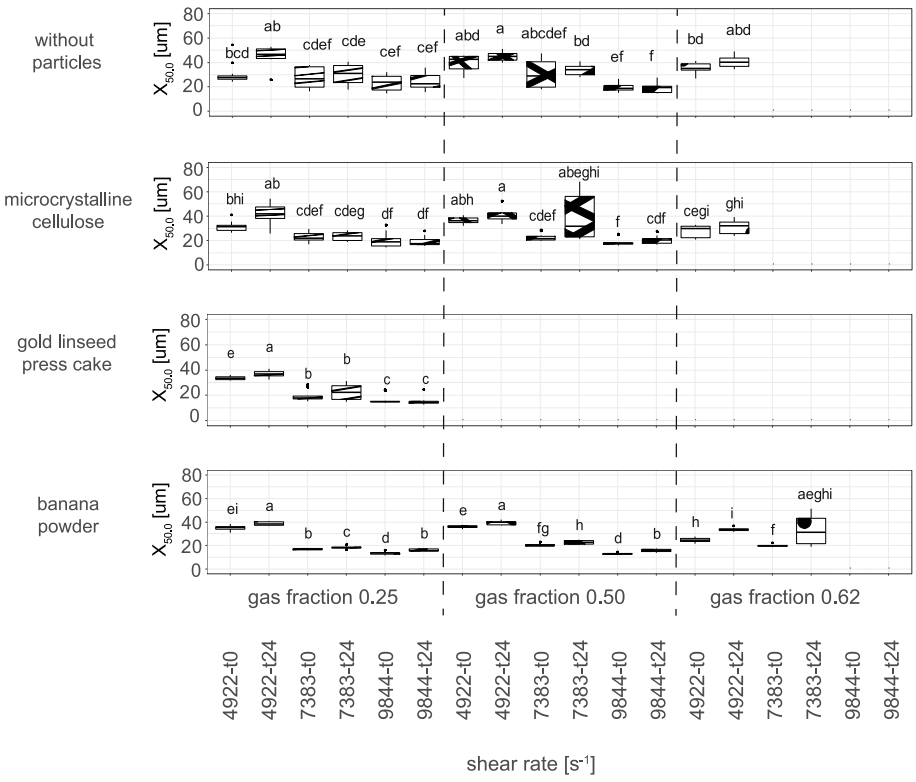

Fig. 3. Bubble size $x_{50.0}$ of particle stabilized foams directly after foaming (t0) and after 24 h storage time at room temperature (t24), n = 12. All tests were carried out with the basic mix with PGE and either without particles (top) or with particles: microcrystalline cellulose (second), gold linseed press cake (third), and banana powder (bottom). The MT-FM foaming unit with the rotor-stator configurations 50/6 was used and a theoretical gas input of 0.25 (left), 0.5 (center), and 0.62 (right), as well as the shear rates 4922, 7383 and 9844 s^{-1}, respectively. Foams were made in duplicate. Letters (a, b, …) indicate classes of significance based on the analysis through a Kruskal-Wallis test (α = 0.05) followed by an unpaired Wilcoxon test using statistical software (RStudio V 1.4 1717, Boston MA, US).

3.2. Influence of foaming machines

The comparison of the foams made with different foaming machines showed a significant difference in terms of bubble size $x_{50.0}$, whereby, the foams produced with the MT-MM led to larger bubble sizes than foams produced with MT-FM. (Fig. 2). The differences in the bubble size $x_{50.0}$ are consistent with observations from several studies (Kempin, Kraume, & Drews, 2020; Kroezen, Groot Wassink, & Schipper, 1988; Müller-Fischer & Windhab, 2005; Rodgers & Cooke, 2012; Utomo, Baker, & Pacek, 2009) and can be attributed to the prevailing shear forces during foaming (MT-FM = 9844 s^{-1}; MT-MM = 4869 s^{-1}). However, the comparison of pure shear force is questionable in the current case. While the shear fields in the rotor-stator and rotating membrane device differ from each other, a mainly turbulent flow field can be expected in the rotor-stator system compared to a laminar flow field with superimposed Taylor vortices in the rotating membrane system (Håkansson, 2018; Müller-Fischer, Bleuler, & Windhab, 2007). What is evident, however, is the influence on the bubble size of PGE in the basic mix, independent of the foaming machine and the additional use of microcrystalline cellulose. As already seen in Fig. 1, PGE leads to significantly lower $x_{50.0}$ and $x_{90.0}/x_{10.0}$ values in most cases with the exception being the foam produced with PGE but without particle addition in the MT-MM.

In terms of drainage, the foams without PGE proved to be extremely unstable, with the foams produced in the MT-MM having completely collapsed after 24h (= 100% drainage) (Fig. 2, bottom graph) and the foams produced in the FT-FM having nearly collapsed with a drainage of 98% and 94%. In contrast, the foams with PGE but no particles proved to be more stable over the same storage time, with lower amounts of drainage found for the foams produced in the rotor-stator machine MT-FM. A distinct increase in foam stability and reduction in drainage is seen for both processes when PGE and the particles, in this case microcrystalline cellulose, are combined. This is in line with previous findings that the combination of fast acting emulsifiers and strong stabilization through particle stabilization results in superior foam stability (Kostakis et al., 2007).

3.3. Influence of foaming parameters

In general, the use of particles led to a reduction in the initial bubble size $x_{50.0}$ (t0) compared to the reference foam without particles (Ref_PGE), especially in foaming processes with high shear rates (7383 s^{-1}, 9844 s^{-1}) (Fig. 3). The lower the shear rate, the more indistinct the differences became, regardless of the gas input or the particles used. This suggests that in foams exposed to a lower shear rate, the bubble formation through the reduction in surface tension achieved by the addition of PGE as an emulsifier is dominant and the particles may be partially dispersed in the continuous phase without interfacial adsorption (Langevin, 2000).

Furthermore, it was found that bubble sizes $x_{50.0}$ were lower at higher shear rates, which is in line with previous findings (Hanselmann & Windhab, 1998; Müller-Fischer, Suppiger, & Windhab, 2007; Pokorny. 2017). It also appears that the bubble size $x_{50.0}$ of foams produced at a shear rate of 9844 s^{-1} tend to have less bubble growth over storage times of 24 h. This can be explained by the fact that foams with smaller initial bubbles are generally less prone to bubble ripening, unless they are too small for the given foam system and shrink before the particles can adsorb for stabilization.

Based on Fig. 3, no clear statement can be made about the influence of the gas input on the initial $x_{50.0}$ value (t0). Going from low to high gas fractions, several effects are superimposed, the main two are that the viscosity of a foam increases with its gas fraction, resulting in higher disruptive shear stresses, while the probability of gas bubbles meeting and coalescing is also enhanced (Müller-Fischer, Bleuler, & Windhab, 2007). There is a tendency that most foams produced with a low gas input (0.25) are subject to more bubble growth during a storage time of 24 h than the foams with a higher gas input (0.5 or 0.62). This tendency can to some extent be explained by the higher viscosity of foams with high gas volume fractions, which slow dissociative effects down.

At higher shear rates gas holding capacity was reduced, resulting in blowby. For example, with the gold linseed press cake particles, foaming was only possible with a gas input of 0.25 at all three shear rates investigated. This might be caused by an increased tendency for the

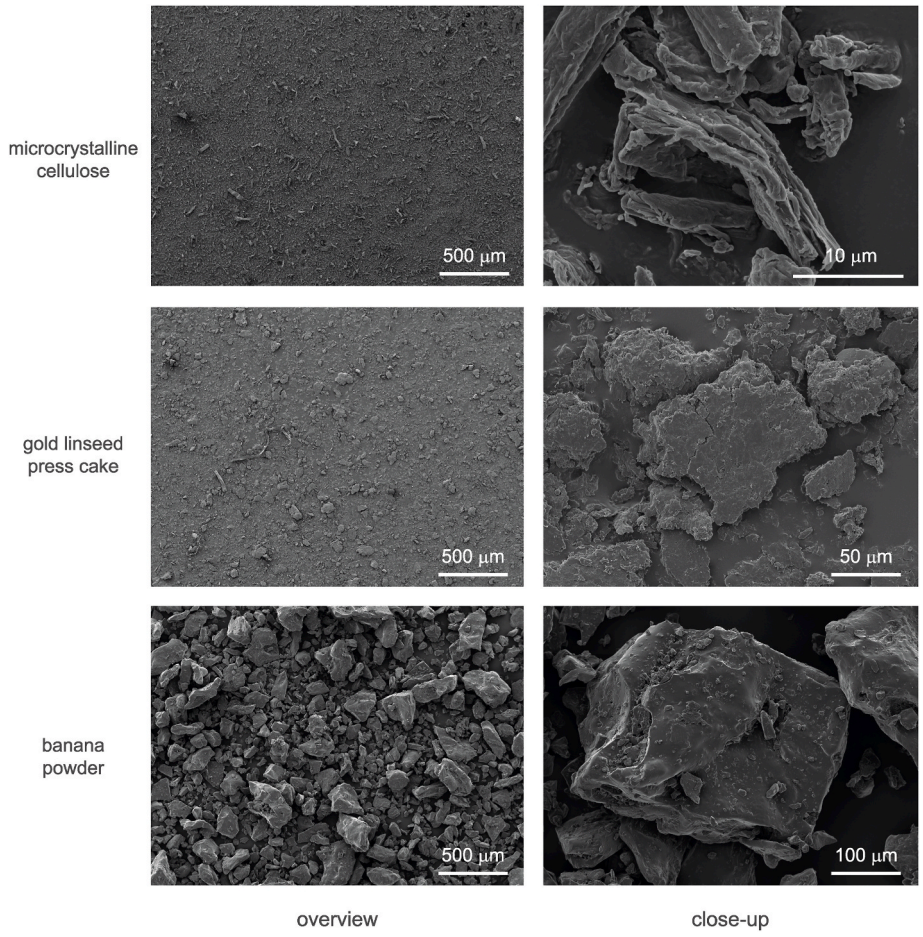

Fig. 4. Scanning electron images of the microcrystalline cellulose (top), gold linseed press cake (middle) and banana powder (bottom) particles in overview (left) and close up view (right).

particle containing suspension to separate into shear fields compared to recipes where all components are similar in density or dissolved. Larger and more rounded shaped particles, such as banana powder and gold linseed press cake, might have a greater effect on such a separation mechanism than smaller particles like microcrystalline cellulose which are smaller and more elongated (Fig. 4). Furthermore, the cohesiveness of gold linseed press cake, which is visible in Fig. 4, might negatively affect the homogeneity of the continuous phase. The smallest initial bubble size $x_{50.0}$ (0h) was recorded in foams with banana powder, produced with a gas input of 0.5 using a shear rate of 9844 s^{-1} (Fig. 3).

The correlation matrix (Fig. 5) shows that the influence of all evaluated particle properties on the bubble size $x_{50.0}$ is relatively small, even though the weak negative linear correlations of particle density and wetting angle were slightly higher after 24 h. However, an increase in these two particle properties is slightly more strongly correlated with a wider bubble size distribution $x_{90.0}/x_{10.0}$, while an increase in BET surface leads to a comparable negative correlation. No correlation between particle size and bubble sizes was found, which is to some extent explainable since all particles are in the same order of magnitude (banana powder 5.5 µm, golden linseed press cake 2.9 µm, microcrystalline cellulose 2.8 µm). In line with findings of various studies (e.g. Costa et al., 2018), the resulting bubble diameters $x_{50.0}$ were about ten-fold larger than the particles used. Nevertheless, some effect on bubble size of the different particle sizes was expected. As the correlation matrix did not show any correlation between particle size and bubble size, it is likely that other particle properties, such as shape, surface structure, swelling capacity or solubility in the aqueous phase, influence the effectiveness of the different particles on gas bubble stability. There is a strong negative linear correlation between drainage and particle size, particle density and the wetting angle: the larger the particles, the greater their density or the higher their wetting angle, the less drainage was observed after 24 h. Looking more closely at the wetting angle, values varied between 27.5 +- 4.0° for microcrystalline cellulose, 53.1°+- 1.6° for banana powder and 74.8 +- 1.6° for golden linseed press cake particles. Hence, drainage was reduced at wetting angles close to 90°, which corresponds well with the fact that an optimum particle wetting angle of 90° leads to increased stability between the interfaces (Fameau & Salonen, 2014; Stocco et al., 2011) as more energy is necessary to detach the particles from the bubble surface (Binks, 2002). The positive effect of a higher particle density and a small BET surface area on drainage cannot be explained at this time. It is suspected that effects of measured particle properties could be overridden by the impact of unmeasured properties, such as viscosity changes in the foam due to the use of particles. Since only the sum of the particle properties allows meaningful conclusions regarding the suitability of individual particle types for foam stabilization to be drawn, the particle types were also correlated with the bubble size $x_{50.0}$, the bubble size distribution $x_{90.0}/x_{10.0}$ and the drainage. There is no evidence to suggest either a positive or negative correlation between particle types used and bubble properties, but it can be stated that the reference foam without particles exhibited in a weak positive correlation and, therefore, a bigger $x_{50.0}$ value. While the microcrystalline cellulose particles correlate to increased drainage, the use of golden linseed press cake and banana powder were found to reduce drainage, with banana powder appearing to be the most effective in achieving foam stability, with a mid-range negative linear correlation of −0.65. The matrix further validates the

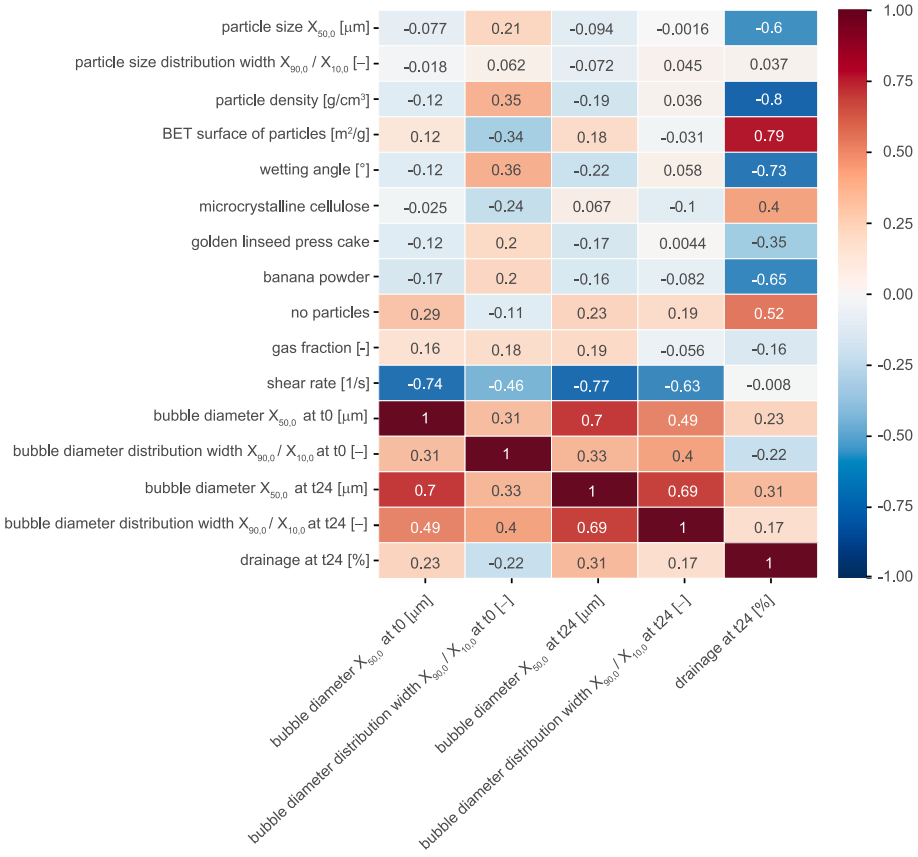

Fig. 5. Correlation matrix for bubble size $x_{50.0}$ and bubble distribution width ($x_{90.0}/x_{10.0}$) for different foaming parameters. All tests were carried out with the basic mix with PGE and banana powder, microcrystalline cellulose and oil press cake gold linseed particles in the MT-FM foaming unit with the rotor-stator configurations 50/2 and 50/6, theoretical gas inputs of 0.25, 0.5 and 0.62 and shear rates 4922, 7383 and 9844 s^{-1}. Correlation coefficients were interpreted as follows: 0 = no linear correlation; 0.3 = weak positive linear correlation; 0.5 = medium strong positive linear correlation; 0.8 = strong positive linear correlation; −0.3 = weak negative linear correlation; −0.5 = medium strong negative linear correlation; −0.8 = strong negative linear correlation.

process parameters studied. Shear rate had the largest negative linear correlation to both bubble size $x_{50.0}$ and bubble distribution width $x_{90.0/x10.0}$. The higher the shear rate, the narrower the bubble size distribution and the smaller the bubble size, which has also been observed in other studies (Kempin et al., 2020; Kroezen et al., 1988; Müller-Fischer & Windhab, 2005; Rodgers & Cooke, 2012; Utomo et al., 2009). Regarding the gas fraction, no comparable correlation could be found. The bubble distribution width $x_{90.0}/x_{10.0}$ at time t0 shows a weak (0.31) positive linear correlation with increased initial bubble size $x_{50.0}$ and the dependence increases slightly after 24 h (0.49). It is also evident that a larger initial $x_{50.0}$ has a strong positive correlation with a higher $x_{50.0}$ value after 24 h, which in turn may favor drainage since the positive correlation increases from 0.23 to 0.31 during storage.

4. Conclusions

This study provides a brief introduction to the manufacturing technologies of particle-stabilized foams and how they are affected by particle characteristics. Based on the results generated, it can be stated that individual particle properties investigated had hardly any detectable influence on bubble quality, but, can strongly improve foam stability. Of the particles investigated, banana powder proved to be the most promising material, firstly in terms of the foam characteristics achieved, and secondly in terms of its suitability for use in foods with clean label requirements. The results obtained confirmed that the rotor-stator foaming technique has a positive effect on bubble quality and on foam stability. Turbulent flow and intensive shearing increased the adsorption energy and thus reduced the initial bubble size and bubble size distribution width, which correlated with reduced drainage. It is anticipated that the potential of particle-stabilized foams will receive more attention in the near future and play an important role in tailoring structural properties in wide range of food applications.

CRediT authorship contribution statement

Ramona Rüegg: Writing – original draft, Writing – review & editing, Investigation. **Tamara Schmid:** Project administration, Methodology, Investigation, Resources, Data curation. **Lukas Hollenstein:** Software, Formal analysis, Data curation, data transformation, data 3+ analysis. **Nadina Müller:** Conceptualization, Visualization, Supervision, Funding acquisition.

Declaration of competing interest

The authors declare no conflict of interest.

Acknowledgments

This study was kindly supported by the financial support of the Swiss Agency for the Promotion of Innovation Innosuisse, Switzerland (project number 40583.1 IP-LS).

References

Aktas, Z., Cilliers, J. J., & Banford, A. W. (2008). Dynamic froth stability: Particle size, airflow rate and conditioning time effects. *International Journal of Mineral Processing, 87*(1–2), 65–71. https://doi.org/10.1016/j.minpro.2008.02.001

Alargova, R. G., Warhadpande, D. S., Paunov, V. N., & Velev, O. D. (2004). Foam superstabilization by polymer microrods. *Langmuir, 20*, 10371–10374. https://doi.org/10.1021/la048647a

Binks, P. B. (2002). Particles as surfactants -similarities and differences. *Current Opinion in Colloid & Interface Science, 7*, 21–41. https://doi.org/10.1016/S1359-0294(02)00008-0

Binks, B. P., & Horozov, T. S. (2005). Aqueous foams stabilized solely by silica nanoparticles. *Angewandte Chemie International Edition in English, 44*(24), 3722–3725. https://doi.org/10.1002/anie.200462470

Colin, A. (2012). Coalescence in foams. In P. Stevenson (Ed.), *Foam engineering: Fundamentals and applications* (pp. 75–90). https://doi.org/10.1002/9781119954620.ch5

Costa, A. L. R., Gomes, A., Tibolla, H., Menegalli, F. C., & Cunha, R. L. (2018). Cellulose nanofibers from banana peels as a Pickering emulsifier: High-energy emulsification processes. *Carbohydrate Polymers, 194*, 122–131. https://doi.org/10.1016/j.carbpol.2018.04.001

Dickinson, E. (2012). Use of nanoparticles and microparticles in the formation and stabilization of food emulsions. *Trends in Food Science & Technology, 24*(1), 4–12. https://doi.org/10.1016/j.tifs.2011.09.006

Dickinson, E. (2015). Structuring of colloidal particles at interfaces and the relationship to food emulsion and foam stability. *Journal of Colloid and Interface Science, 449*, 38–45. https://doi.org/10.1016/j.jcis.2014.09.080

Du, Z., Bilbao-Montoya, M. P., Binks, B. P., Dickinson, E., Ettelaie, R., & Murray, B. S. (2003). Outstanding stability of particle-stabilized bubbles. *Langmuir, 19*(8), 3106–3108. https://doi.org/10.1021/la034042n

E, X., Pei, Z. J., & Schmidt, K. A. (2010). Ice cream: Foam formation and stabilization – a review. *Food Reviews International, 26*(2), 122–137. https://doi.org/10.1080/87559120903564472

Fameau, A.-L., & Salonen, A. (2014). Effect of particles and aggregated structures on the foam stability and aging. *Comptes Rendus Physique, 15*(8–9), 748–760. https://doi.org/10.1016/j.crhy.2014.09.009

Fujii, S., Iddon, P. D., Ryan, A. J., & Armes, S. P. (2006). Aqueous particulate foams stabilized solely with polymer latex particles. *Langmuir, 22*(18), 7512–7520. https://doi.org/10.1021/la060812u

Gonzenbach, U. T., Studart, A. R., Tervoort, E., & Gauckler, L. J. (2006). Macroporous ceramics from particle-stabilized wet foams. *Journal of the American Ceramic Society, 90*(1), 16–22. https://doi.org/10.1111/j.1551-2916.2006.01328.x

Guevara, J. S., Mejia, A. F., Shuai, M., Chang, Y.-W., Mannan, M. S., & Cheng, Z. (2012). Stabilization of Pickering foams by high-aspect-ratio nano-sheets. *Soft Matter, 9*(4), 1327–1336. https://doi.org/10.1039/C2SM27061G

Håkansson, A. (2018). Rotor-stator mixers: From batch to continuous mode of operation—a review. *Processes, 6*(4), 32. https://doi.org/10.3390/pr6040032

Hanselmann, W., & Windhab, E. (1998). Flow characteristics and modelling of foam generation in a continuous rotor/stator mixer. *Journal of Food Engineering, 38*(4), 393–405. https://doi.org/10.1016/S0260-8774(98)00129-0

Ho, T. M., Le, T. H. A., Yan, A., Bhandari, B. R., & Bansal, N. (2019). Foaming properties and foam structure of milk during storage. *Food Research International, 116*, 379–386. https://doi.org/10.1016/j.foodres.2018.08.051

Hunter, T. N., Pugh, R. J., Franks, G. V., & Jameson, G. J. (2008). The role of particles in stabilising foams and emulsions. *Advances in Colloid and Interface Science, 137*(2), 57–81. https://doi.org/10.1016/j.cis.2007.07.007

Hutzler, S., Weaire, D., Saugey, A., Cox, S., & Peron, N. (2005, October). *The physics of foam drainage. 52*. Würzburg, DE: *SEPAWA Kongress mit Europ*ean detergents conference.

Kalashnikova, I., Bizot, H., Bertoncini, P., Cathala, B., & Capron, I. (2013). Cellulosic nanorods of various aspect ratios for oil in water Pickering emulsions. *Soft Matter, 9*(3), 952–959. https://doi.org/10.1039/c2sm26472b

Kapatay, G., & Babcsán, N. (2012). Particle stabilized foams. In P. Stevenson (Ed.), *Foam engineering: Fundamentals and applications* (pp. 122–138).

Kaptay, G. (2003). Interfacial criteria for stabilization of liquid foams by solid particles. *Colloids and Surfaces A: Physicochemical and Engineering Aspects, 230*(1–3), 67–80. https://doi.org/10.1016/j.colsurfa.2003.09.016

Kempin, M. V., Kraume, M., & Drews, A. (2020). W/O Pickering emulsion preparation using a batch rotor-stator mixer – influence on rheology, drop size distribution and filtration behavior. *Journal of Colloid and Interface Science, 573*, 135–149. https://doi.org/10.1016/j.jcis.2020.03.103

Koehler, S. A. (2012). Foam drainage. In P. Stevenson (Ed.), *Foam engineering: Fundamentals and applications* (pp. 27–58).

Kostakis, T., Ettelaie, R., & Murray, B. S. (2007). Enhancement of stability of bubbles to disproportionation using hydrophilic silica particles mixed with surfactants or proteins. In E. Dickinson, & M. E. Leser (Eds.), *Food colloids: Self-assembly and material science* (pp. 357–368).

Kroezen, A. B. J., Groot Wassink, G., & Schipper, C. A. C. (1988). The flow properties of foam. *Journal of the Society of Dyers and Colourists, 104*(10), 393–400. https://doi.org/10.1111/j.1478-4408.1988.tb01138.x

Langevin, D. (2000). Influence of interfacial rheology on foam and emulsion properties. *Advances in Colloid and Interface Science, 88*(1–2), 209–222. https://doi.org/10.1016/s0001-8686(00)00045-2

Madivala, B., Vandebril, S., Fransaer, J., & Vermant, J. (2009). Exploiting particle shape in solid stabilized emulsions. *Soft Matter, 5*(8). https://doi.org/10.1039/b816680c

Martínez-Flores, H. E., Barrera, E. S., Garnica-Romo, M. G., Penagos, C. J. C., Saavedra, J. P., & Macazaga-Alvarez, R. (2006). Functional characteristics of protein flaxseed concentrate obtained applying a response surface methodology. *Journal of Food Science, 71*(8), C495–C498. https://doi.org/10.1111/j.1750-3841.2006.00147.x

Müller-Fischer, N., Bleuler, H., & Windhab, E. J. (2007b). Dynamically enhanced membrane foaming. *Chemical Engineering Science, 62*, 4419. https://doi.org/10.1016/j.ces.2007.05.026

Müller-Fischer, N., Suppiger, D., & Windhab, E. J. (2007a). Impact of static pressure and volumetric energy input on the microstructure of food foam whipped in a rotor–stator device. *Journal of Food Engineering, 80*(1), 306–316. https://doi.org/10.1016/j.jfoodeng.2006.05.026

Müller-Fischer, N., & Windhab, E. J. (2005). Influence of process parameters on microstructure of food foam whipped in a rotor–stator device within a wide static pressure range. *Colloids and Surfaces A: Physicochemical and Engineering Aspects, 263*(1), 353–362. https://doi.org/10.1016/j.colsurfa.2004.12.057

Pokorny, L. (2017). *Dynamic membrane aeration processing of novel micro-structure in water- and fat-continuous multiphase food systems*. Doctoral Thesis. ETH Zurich. https://doi.org/10.3929/ethz-b-000265805.

Rayner, M. (2015). Current status on novel ways for stabilizing food dispersions by oleosins, particles and microgels. *Current Opinion in Food Science, 3*, 94–109. https://doi.org/10.1016/j.cofs.2015.05.006

Rodgers, T. L., & Cooke, M. (2012). Rotor–stator devices: The role of shear and the stator. *Chemical Engineering Research and Design, 90*(3), 323–327. https://doi.org/10.1016/j.cherd.2011.07.018

Saint-Jalmes, A. (2006). Physical chemistry in foam drainage and coarsening. *Soft Matter, 2*(10), 836–849. https://doi.org/10.1039/b606780h

Stocco, A., Drenckhan, W., Rio, E., Langevin, D., & Binks, B. P. (2009). Particle-stabilised foams: An interfacial study. *Soft Matter, 5*(11), 2215–2222. https://doi.org/10.1039/B901180C

Stocco, A., Rio, E., Binks, B. P., & Langevin, D. (2011). Aqueous foams stabilized solely by particles. *Soft Matter, 7*(4), 1260–1267. https://doi.org/10.1039/C0SM01290D

Tang, F. Q., Xiao, Z., Tang, J. A., & Jiang, L. (1989). The effect of SiO_2 particles upon stabilization of foam. *Journal of Colloid and Interface Science, 131*(2), 498–502. https://doi.org/10.1016/0021-9797(89)90192-6

Utomo, A., Baker, M., & Pacek, A. W. (2009). The effect of stator geometry on the flow pattern and energy dissipation rate in a rotor–stator mixer. *Chemical Engineering Research and Design, 87*(4), 533–542. https://doi.org/10.1016/j.cherd.2008.12.011